Ferrimagnetic magnon drop solitons close to the angular momentum compensation point

C. E. Zaspel,[1] E. G. Galkina,[2] and B. A. Ivanov[3,4]

[1]*Department of Environmental Science, University of Montana-Western, Dillon, Montana 59725, USA*
[2]*Institute of Physics, National Academy of Science of Ukraine, 03142 Kiev, Ukraine*
[3]*Institute of Magnetism, National Academy of Science of Ukraine, 03142 Kiev, Ukraine*
[4]*Institute for Molecules and Materials, Radboud University Nijmegen, Nijmegen 6525XZ, The Netherlands*

(Received 16 May 2023; revised 14 July 2023; accepted 21 July 2023; published 3 August 2023)

Precessional solitons, referred to as magnon drop solitons driven by spin torque, are known to exist in ferromagnetic free layers of nanocontact devices. To increase the operating frequency of nanoscale devices, it has been proposed that transition metal–rare earth ferromagnetic alloys are good candidates. In addition, these alloys can exhibit angular momentum compensation providing another parameter controlling frequency. In this article magnon drop solitons in ferrimagnets are studied by a combination of analytical and numerical solutions of the Landau-Lifshitz equation for a two-sublattice model. For such magnets, two magnon modes exist, but only one of them, the mode with the lower absolute value of the precession frequency, is involved in the formation of the droplike soliton. The precession frequency for the soliton depends strongly on the angular momentum compensation parameter; it grows significantly in the vicinity of the angular momentum compensation point. These solitons are shown to be stable and a minimum sustainable compensation-dependent spin torque is obtained.

DOI: 10.1103/PhysRevB.108.064403

I. INTRODUCTION

The soliton-based approach is the most suitable for the description of physical systems with essentially nonlinear dynamics, for example, magnetically ordered materials. This approach is well suited for investigation of static and dynamic solutions of the Landau-Lifshitz equation, describing nonlinear spin dynamics of ferromagnets [1–9]. Originally low-dimensional topological and nontopological magnetic solitons such as vortices, skyrmions, and magnon drops of various dimensions were of interest to theorists as brief examples of highly nonlinear elementary excitations. With the development of nanoscale fabrication technology, solitons were experimentally observed in structures such as nanodisks [10,11] and nanocontacts [12,13] on a thin ferromagnetic film. The dynamic properties of magnetic vortices typically involve frequencies in the sub-GHz to low-GHz range, so an obvious application of magnetic solitons is high-frequency nanoscale oscillators [14,15]. For oscillator applications, the theoretical development of spin transfer torque has been shown to provide the necessary driving force for excitation of soliton dynamics. Subsequently, nanopillar and nanocontact devices have been fabricated for nanoscale oscillator applications based on magnetic vortex dynamics.

For nanoscale oscillator applications it is desirable to further increase the operating frequency, which is limited by the magnetic properties of the free-layer material. A typical free-layer material can be a ferromagnetic alloy such as permalloy, but this alloy limits the highest frequency to about 1 GHz for a magnetic vortex oscillator. Recently it was shown that various dynamical processes, in particular, the operating frequency of spin-pumped nano-oscillators, can be significantly increased to the subterahertz range using a ferrimagnetic transition metal–rare earth (TM-RE) free layer such as alloy Gd(Co,Fe) close to the angular momentum compensation point [16–19].

It is important to stress that some ferrimagnetic materials can have so-called compensation points, where either the magnetizations or angular momenta of sublattices compensate each other at some temperature values. Generally, these two temperatures are not equal and their difference can be as large as 50 K [16]. The key point here is that near the compensation of the angular momenta (at the angular momentum compensation point) the spin dynamics becomes faster [16–21]. Moreover, angular momentum compensated ferrimagnetic alloys can have a nonzero magnetic moment resulting in the possibility of vortex formation in the free layer. The vortex oscillator frequency can be increased to a range of 10–30 GHz and then controlled by the current as well as alloy concentrations. Also, temperature dependence of the angular momentum and magnetization compensation points implies that temperature has an effect on the frequency [20,21].

In light of the significant increase in the operating frequency range of vortex oscillators in ferrimagnetic layers, it is important to study other forms of solitons in these systems. In this article the nontopological magnon drop soliton driven by spin torque with a nanocontact on a ferrimagnetic alloy is theoretically studied near the angular momentum compensation point. Previous theoretical work on magnon drop solitons [2–9] has been done for ferromagnets by solution of the Landau-Lifshitz-Gilbert (LLG) equation. In these systems magnon drops form in perpendicular easy-axis ferromagnets with the central magnetization nearly opposite the free-layer magnetization with a relatively narrow transition region defining the soliton edge. Without Gilbert damping, solution of the LL equation results in a so-called conservative magnon

drop stabilized by precession of the magnetization. It is worth mentioning here the origin of such terminology: in the framework of quantum mechanics, these solitons can be treated as a bound state of a large number of magnons; thus this soliton resembles the drop of usual liquid with magnons as the strongly interacting particles in liquid [2]. With the addition of nonconservative terms in the LLG equation, spin torque will provide necessary antidamping for the formation of a dissipative droplet soliton. This type of soliton can exist because dissipation is balanced by spin torque resulting in a structure stabilized by dynamic precession. The magnon drop soliton has been experimentally observed [22–24] in ferromagnetic free-layer systems having high precession frequencies in the range 10–20 GHz. Since ferromagnetic magnon drop solitons result in a high oscillator operating frequency, and ferrimagnetic dynamics can result in a further frequency increase, the goal here is an investigation of the modified LLG equation describing ferrimagnetic dynamics close to the angular momentum compensation point.

To determine magnon drop soliton structures, precession frequencies, and stability, this paper is organized as follows: First the modified LLG equation including spin torque is presented for the ferrimagnet in the vicinity of the angular momentum compensation point. For the special case of the conservative magnon drop without damping and spin torque the form of the conservative soliton is determined numerically to obtain the precession frequencies and radial structures as a function of the boundary condition at the nanocontact center. The interesting result here is the relation between the precession frequency and angular momentum compensation parameter. These compensation-dependent solutions are then used to calculate quantities such as the precession frequency and the total magnetization of the free layer. Finally, on the basis of soliton perturbation theory, the time dependence of the total magnetization is used to investigate the effect of damping and spin torque on the stability of these solutions.

II. FERRIMAGNETIC DYNAMICS

We begin with a definition of the variables and parameters used in the LLG equation driven by spin torque. In addition, the approximations leading to the magnon drop solutions of the LLG equation are outlined. For a two-sublattice ferrimagnet the magnetizations are expressed as $\vec{M}_{1,2} = g_{1,2}\mu_B\vec{s}_{1,2}$ in terms of the sublattice g values and spin densities, where μ_B is the Bohr magneton. The lengths of sublattice spins have different dependence on the temperature, and at some value of the temperature (angular momentum compensation point) they can be equal, giving rise to angular momentum compensation. It is worth noting here that g factors of sublattices usually are not equal: the compensation of magnetizations takes place at some different temperature (magnetization compensation point), where the effects of the increased frequency spin dynamics are absent; see, e.g., [16,17,20,25]. Close to the angular momentum compensation point, $\vec{s}_1 + \vec{s}_2 \approx 0$, so it is sufficient to use the formulation for the antiferromagnet with variables, normalized total density of angular momentum $\vec{m} = \frac{\vec{s}_1+\vec{s}_2}{2s_0}$, and the so-called antiferromagnetic vector, or Néel vector $\vec{l} = \frac{\vec{s}_1-\vec{s}_2}{2s_0}$. In the following $s_{1,2} = |\vec{s}_{1,2}|$ and $s_0 = (s_1 + s_2)/2$ unless the vector notation is explicitly given. Then in the continuum approximation the free-layer energy density is

$$w = \frac{E_{\text{ex}}}{2}\vec{m}^2 + \frac{A}{2}(\nabla\vec{l})^2 + \frac{K}{2}\left(1 - l_z^2\right), \tag{1}$$

where E_{ex} is the homogeneous exchange energy, describing the intersublattice exchange, which is often used to analyze antiferromagnets (see [25] for more details), A is the nonhomogeneous exchange constant, and K is the easy-axis anisotropy constant. Instead of using of the set of Landau-Lifshitz equations for spin densities $\vec{s}_1$ and $\vec{s}_2$ or, equivalently, for the vectors $\vec{m}$ and $\vec{l}$, we use so-called sigma-model approximation, well known for antiferromagnets and valid for ferrimagnets near the compensation point; see [25]. The derivation of the sigma-model equation is based on two conditions: first, that the length of the vector $\vec{m}$ is much less than the length of the vector $\vec{l}$ and, second, that the exchange constant E_{ex} exceeds the value of the anisotropy constant. Within the framework of this approach, the vector $\vec{m}$ can be excluded from the set of equations resulting in one closed equation for the principal dynamic variable, the normalized antiferromagnetic vector $\vec{l}$. The dynamics of $\vec{l}$ is described by the equation

$$\hbar(s_1 - s_2)\frac{\partial\vec{l}}{\partial t} + \hbar(s_1 + s_2)\frac{1}{\omega_{\text{ex}}}\left(\vec{l}\times\frac{\partial^2\vec{l}}{\partial^2 t}\right) = -\vec{l}\times\frac{\delta W}{\delta\vec{l}}, \tag{2}$$

where $W = W(\vec{l})$ is the static energy of the ferrimagnet, written as a functional of the vector function $\vec{l}$, and $\hbar\omega_{\text{ex}} = g\mu_B H_{\text{ex}}$, H_{ex} is the so-called exchange field; see monograph by Turov *et al.* [26] for more details. Within this approach, the vector $\vec{m}$ plays the role of a slave variable; it can be expressed through $\vec{l}$ and $\partial\vec{l}/\partial t$ by a simple formula. See, e.g. [25],

$$\vec{m} = \nu\vec{l} + \frac{1}{\omega_{\text{ex}}}\left(\frac{\partial\vec{l}}{\partial t}\times\vec{l}\right), \tag{3}$$

where the compensation parameter $\nu = (s_1 - s_2)/(s_1 + s_2)$ is introduced. This parameter shows how far from the compensation point the ferrimagnet is, and at the angular momentum compensation point the compensation parameter $\nu = 0$. Thus, instead of two equations for the sublattice magnetizations, one equation can be used for the antiferromagnetic vector $\vec{l}$. Note that far from the compensation point, where $\nu \sim 1$, the term with the second time derivative in Eq. (2) is a higher-order correction that can be neglected, and the standard first-order Landau-Lifshitz-Gilbert equation for the total spin density of the ferrimagnet is sufficient, which equals $(s_1 - s_2)\vec{l}$; see [25] for more details.

For the case when $l \gg m$ the Landau-Lifshitz equations for each sublattice can be expressed in terms of the single free-layer antiferromagnetic vector, $\vec{l} = (\sin\theta\cos\varphi, \sin\theta\sin\varphi, \cos\theta)$ in polar coordinates with the z axis perpendicular to the free layer and the origin is at the center of the nanocontact. In the following the nonconservative terms are Gilbert damping and spin torque where the spin polarization has the normalized components (p_1, p_2, p_3), and

the equations for the dependent variables, $\theta(\vec{r},t)$ and $\varphi(\vec{r},t)$, are [25]

$$-\nu\sin\theta\dot{\varphi} = \frac{1}{\omega_{\rm ex}}(\ddot{\theta}-c^2\nabla^2\theta)-\frac{1}{\omega_{\rm ex}}\sin\theta\cos\theta[\dot{\varphi}^2-c^2(\nabla\varphi)^2] + \omega_K\sin\theta\cos\theta+\alpha\dot{\theta} - \tau\sin^2\theta(p_2\cos\varphi-p_1\sin\varphi), \quad (4)$$

$$\nu\sin\theta\dot{\theta} = \frac{1}{\omega_{\rm ex}}(\ddot{\varphi}\sin^2\theta+\dot{\theta}\dot{\varphi}\sin 2\theta)-\frac{c^2}{\omega_{\rm ex}}\nabla(\sin^2\theta\nabla\varphi) + \alpha\dot{\varphi}\sin^2\theta+\tau p_3\sin^2\theta + \tau\sin\theta\cos\theta(p_1\cos\varphi+p_2\sin\varphi). \quad (5)$$

Here the dot indicates the time derivative, α is the Gilbert damping constant ($\alpha\cong 0.01$), $\tau=\sigma j$ is the spin-torque term where $\sigma=\frac{\epsilon g\mu_B}{2eLM_s}$, and j is the nanocontact current density in a free layer of the thickness L. Additional parameters are defined to be the exchange frequency, $\omega_{\rm ex}$, anisotropy frequency, ω_K, and the characteristic magnon velocity c; see [21,25] for details.

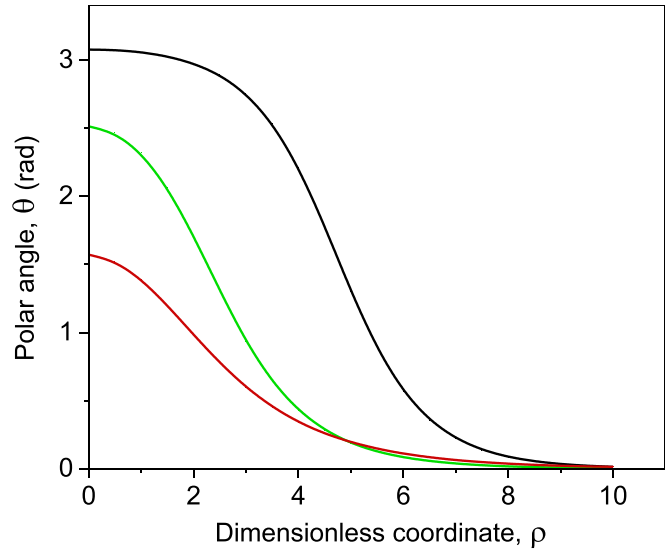

FIG. 1. Radial soliton profiles with $\theta(0)=0.98\pi$ (black), $\theta(0)=0.80\pi$ (green), and $\theta(0)=0.50\pi$ (red).

III. CONSERVATIVE MAGNON DROP

Without damping and spin torque the form of the conservative droplet solution is obtained through the ansatz, $\varphi=-\omega t$ and $\theta=\theta(r)$ with $\alpha=0$ and $\tau=0$. Note the negative sign in the time dependence of φ, which is opposite to that used before for ferromagnetic droplets. This difference is because in the earlier papers the Landau-Lifshitz equation for magnetization was used, whereas here we are using equations for spin density, which has the opposite sign. Then Eq. (5) is satisfied automatically and Eq. (4) simplifies to a standard [2–6] form,

$$\nabla_\rho^2\theta-\sin\theta\cos\theta+\Omega\sin\theta=0, \quad (6)$$

in terms of the dimensionless length and frequency parameters $\rho=r/a$ where $a^2=c^2/\omega_K\omega_{\rm ex}(1-\bar{\omega}^2)$ and $\Omega=\bar{\nu}\bar{\omega}/(1-\bar{\omega}^2)$. It is quite natural to introduce dimensionless frequency $\bar{\omega}=\omega/\sqrt{\omega_{\rm ex}\omega_K}$, because the quantity $\sqrt{\omega_{\rm ex}\omega_K}$ coincides with the "exchange-enhanced" frequency of linear magnetic resonance exactly at the angular momentum compensation point $\nu=0$ [18,25]. With the parameters applicable to Gd(Fe,Co), the values are $\omega_{\rm ex}/2\pi=5$ THz and $\omega_K/2\pi=2.8$ GHz with a corresponding spin density, $\sqrt{\omega_{ex}\omega_K}=118$ rad/ns. The minimal value for a is $c/\sqrt{\omega_{\rm ex}\omega_K}$, which can be rewritten as $\sqrt{A/K}=8.6$ nm using values of $A=5.2\times10^{-12}$ J/m, $K=70$ kJ/m^3 [27], and $c=6$ km/s. Note that in the notation of Eq. (1) these values are twice as large as those in [27] because of different definitions. Also, the use of the reduced compensation parameter, $\bar{\nu}=\nu\sqrt{\omega_{\rm ex}/\omega_K}\gg\nu$, is quite natural for the case of interest, i.e., almost-compensated ferrimagnets with $\nu\ll1$; see [18,21,25,28].

Soliton solutions are obtained by numerical integration of Eq. (6) using the shooting method with the boundary conditions, $\theta(r)|_{r=0}=\theta(0)$, $d\theta(r)/dr|_{r=0}=0$, and $\theta(r)\to0$ as $r\to\infty$, which also gives a numerical value for the parameter Ω at given value of $\theta(0)$ and vice versa. It is further remarked that the magnon drop solution only exists if $1>\Omega>0$; see [2–6]. The solutions of Eq. (6) for the case of a ferromagnet have been known [2–6] for many years with a characteristic linear relation between Ω and the precession frequency, ω. However, for the ferrimagnet it is noticed that there is a more complicated relation between the parameter Ω and the precession frequency also involving the angular momentum compensation parameter. Typical soliton radial forms are shown in Fig. 1 for different values of $\theta(0)$ where it is remarked that the approximate soliton radius decreases for smaller initial values of $\theta(0)$. At the most interesting case of small values of Ω, the soliton profile is "dropletlike" type, with a large enough central area, where $\theta(r)\sim\pi$, bordered by the "domain wall" from the rest of the magnet, where $\theta(0)\to0$.

Previous numerical simulations [8,9] have shown that the soliton radius tends to match the nanocontact radius with both centers roughly coinciding. These observations indicate that the $\theta(0)$ condition is related to the nanocontact radius.

For the ferromagnet the initial $\theta(0)$ corresponds to a single frequency, but owing to the form of Ω as a function of ω, this is no longer the case for the ferrimagnet. With Ω determined by numerical solution of Eq. (6) it is noticed that two mode frequencies can be obtained in terms of the parameters, Ω,

$$\bar{\omega}=\frac{\omega}{\sqrt{\omega_{\rm ex}\omega_K}}=\frac{1}{2\Omega}(-\bar{\nu}\pm\sqrt{4\Omega^2+\bar{\nu}^2}). \quad (7)$$

It is noted that Eq. (7) implies that there are two solutions; however, owing to the definition of a and the requirement that $0<\Omega<1$, the only frequency corresponding to the upper sign of Eq. (7) must be chosen for the case of magnon drop solitons. In the following only the positive sign will be considered. Using Eq. (7) the positive-frequency branch is plotted versus a reduced compensation parameter, $\bar{\nu}$ for various initial $\theta(0)$, or equivalently Ω in Fig. 2.

In the $\nu\to0$ limit notice that the frequency becomes $\omega^2=\omega_{\rm ex}\omega_K$, giving the frequency characteristic for antiferromagnets. Moreover, the frequency branch of Fig. 2 is a decreasing function of the compensation parameter, which will be of interest in spin-torque oscillator applications. For large values

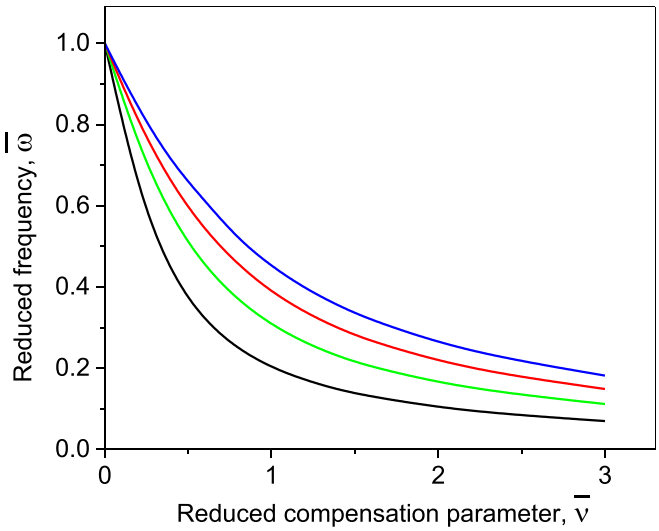

FIG. 2. Reduced frequency $\bar{\omega} = \omega/\sqrt{\omega_{ex}\omega_K}$ versus $\bar{\nu}$ for $\theta(0) = 0.98\pi$ (black), $\theta(0) = 0.9\pi$ (green), $\theta(0) = 0.8\pi$ (red), and $\theta(0) = 0.7\pi$ (blue). Here and in the following figures these correspond to $\Omega = 0.2109$, $\Omega = .3392$, $\Omega = 0.4576$, and $\Omega = 0.5660$, respectively.

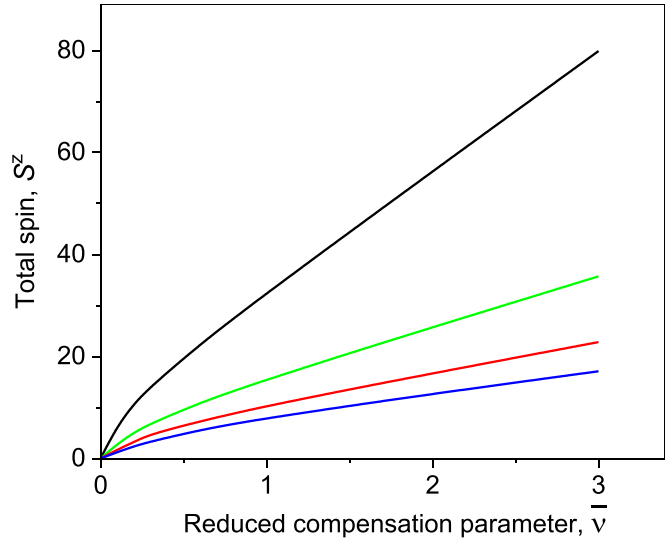

FIG. 3. The total spin, S^z versus $\bar{\nu}$ for $\theta(0) = 0.98\pi$ (black), $\theta(0) = 0.9\pi$ (green), $\theta(0) = 0.8\pi$ (red), and $\theta(0) = 0.7\pi$ (blue). It is noted that the maximum S^z decreases as $\theta(0)$ decreases.

of $\bar{\nu} \gg 1$ the positive-frequency mode has the form $\bar{\omega} = \Omega/\bar{\nu}$ or $\omega = \omega_K\Omega/\nu$, and at the ferromagnetic limit ($\nu = 1$) the positive-frequency mode corresponds to the ferromagnetic soliton. However, at the ferrimagnetic region $\nu \ll 1$ its order of magnitude is determined by the exchange-relativistic quantity $\sqrt{\omega_{ex}\omega_K}$. Note that in this limit the other mode with negative frequency (not corresponding to drop solitons) is $\bar{\omega} = -\bar{\nu}/\Omega$ or $\omega = -\nu\omega_{ex}/\Omega$; which is the exchange mode for the standard ferrimagnet far from the compensation point.

Here we would like to mention one limitation of this theory: In the formal limit $\nu \to 0$ with a finite value of Ω it is noted $\omega \to \sqrt{\omega_{ex}\omega_K}$ and the characteristic soliton size a is divergent. This problem is known for droplet solitons in antiferromagnets [29] (see also the recent review [30]), which can be solved by inclusion of a higher anisotropy term of the form of $-K'(l_x^2 + l_y^2)^2$ with positive constant K'. However, we will not discuss such generalization of the model because we were not able to find any information about such higher anisotropy terms for materials of interest like Gd(FeCo) alloys. This limit will be discussed later during the treatment of nonconservative solitons.

IV. DISSIPATIVE MAGNON DROP

Next, the dynamic effects of damping and spin torque will be determined by an analysis of the time dependence of the free-layer spin components using numerical solutions for the droplet structure $\theta(\rho)$. Previous authors [8] have obtained the sustaining spin torque necessary for magnon drop solitons in ferromagnetic nanocontacts through a linearization of Eq. (2) along with the compatibility condition. However, for the ferrimagnet the parameter $\Omega(\bar{\omega}, \bar{\nu})$ depends on an additional compensation parameter. Here the effect of nonlinearity on the stability and sustaining spin torque is determined from consideration of the time dependence of the dimensionless z component of the spin associated with the soliton S_z, which equals the difference between the total spin of the magnet in the ground state and the soliton total spin [2]. This quantity can be found by $S_z = 2s_0 \int(\nu - m_z)d\boldsymbol{r}$ which is integrated over the area of the film—here $2s_0 m_z$ is the spin density determined by Eq. (3)—and by the definition, the value of S_z is positive. Without accounting for the effects of damping and spin torque, the quantity S_z is conserved. In the general case, the evolution of this quantity can be found by integration of Eq. (5) over the free-layer area to give the key equation used to determine soliton stability,

$$\frac{d}{dt}\int_0^\infty \left[\nu(1-\cos\theta) + \frac{\omega}{\omega_{ex}}\sin^2\theta\right]\varrho d\varrho = \int_0^\infty (-\alpha\omega + \tau p_3)\sin^2\theta\rho d\rho, \tag{8}$$

where $\tau > 0$ and units are GHz. Here the left-hand integrand is proportional to the time derivative of S^z,

$$S^z = \sqrt{\frac{\omega_K}{\omega_{ex}}}\int_0^\infty [\bar{\nu}(1-\cos\theta) + \bar{\omega}\sin^2\theta]\varrho d\varrho, \tag{9}$$

which is clearly conserved in the absence of dissipation and spin torque (to shorten the equation, we omit the multiplier 2π). The z component of the total spin is calculated numerically for the range, $0.01 < \bar{\nu} < 3$, using Eq. (9) for different Ω values with the results shown in Fig. 3.

Using Eq. (8), the time derivative of S^z can be written as

$$\frac{dS^z}{dt} = -\alpha\bar{\omega}\sqrt{\omega_{ex}\omega_K}J + \tau p_3 F. \tag{10}$$

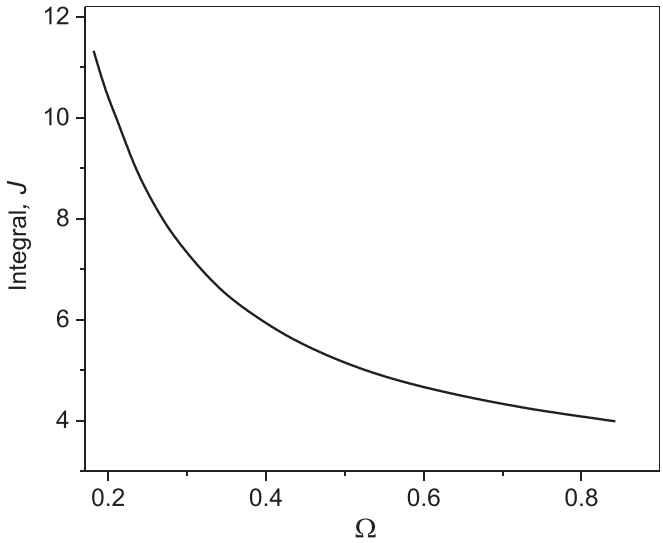

FIG. 4. The integral, $J(\Omega)$ versus parameter Ω in Eq. (6).

Here the functions $J(\Omega)$ and $F(\Omega, \bar{\omega})$ are defined by the integrals,

$$J(\Omega) = \int_0^{\infty} \sin^2\theta(\rho)\rho d\rho, \tag{11}$$

$$F(\Omega, \bar{\omega}) = \int_0^{\rho_0} \sin^2\theta(\rho)\rho d\rho, \tag{12}$$

where the upper limit is $\rho_0 = r_0/a$ and r_0 is the nanocontact radius. Moreover, the upper limit is also a function of $\bar{\omega}$ through the definition of a so the integral defining $F(\Omega, \bar{\omega})$ includes two variables. Finally, the assumption that the radial dependence of τ is represented by a unit step function results in the form of Eq. (12).

In the following the integrals are calculated numerically with $\bar{\omega}(\Omega, \bar{\nu})$ given by Eq. (7) and θ is the numerical solution of Eq. (6). Bear in mind that Ω only depends on the "initial" $\theta(0)$ so in the following the J, F, and S^z integrals are represented by data sets obtained for variable $\theta(0)$ with fixed $\bar{\nu}$ corresponding to measurements on an actual system. This is done for a fixed compensation parameter with a range $0.4\pi < \theta(0) < \pi$ corresponding to $\Omega = 0.8431\pi$ when $\theta(0) = 0.4\pi$ and $\Omega = 0.18181\pi$ for $\theta(0) = 0.99\pi$. Using Eq. (11) the integral $J(\Omega)$ is shown in Fig. 4. It is remarked that this integral is dependent of $\bar{\nu}$ or $\bar{\omega}$ only through their combination, Ω.

Referring to Eq. (10) it is natural to choose S^z as the independent variable for stability analysis so both F and $\bar{\omega}$ are expressed in terms of this variable with the results shown in Figs. 5 and 6 for reduced compensation parameters in the range $0.1 \leqslant \bar{\nu} \leqslant 1$.

The limiting behavior in Figs. 5 and 6 can be understood in terms of $\theta(0)$. In the limit $\theta(0) \to 0$ the limits of the other quantities are $\bar{\omega} \to 1$, $S^z \to 0$ from Eq. (9) and since $a \to \infty$, the upper limit in Eq. (12), $\rho_0 \to 0$, and the integral, $F \to 0$. In the more interesting limit $\theta(0) \to \pi$, the value of $\bar{\omega} \to 0$, $\cos\theta \cong -1$, and the well-defined droplike form of the soliton with a circular domain wall of the radius $R \gg a$ is forming (see Fig. 1 and [2,6] for details); in this case the value of $S^z \to \infty$. When the value of R exceeds the contact radius, since $\sin\theta \cong 0$ in the nanocontact area, $F \to 0$ as seen in Fig. 6.

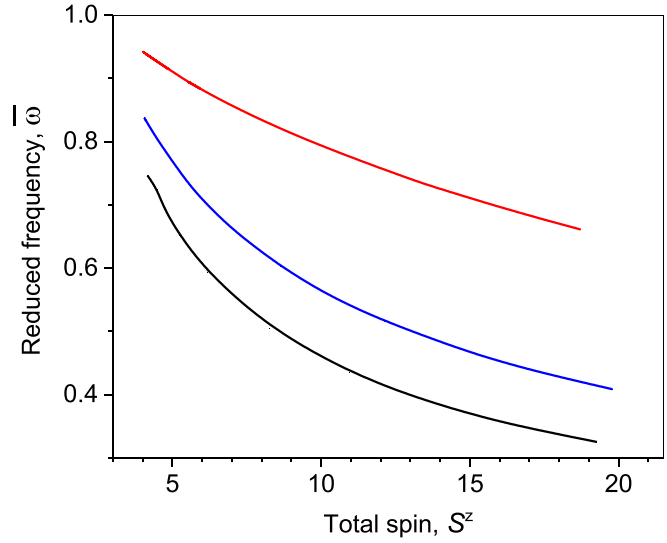

FIG. 5. Reduced frequency of the spin precession in the soliton $\bar{\omega}$, defined by Eq. (7), versus S^z; $\bar{\nu} = 1$ (black), $\bar{\nu} = 0.1$ (red), $\bar{\nu} = 0.5$ (blue), and $\bar{\nu} = 0.1$ (red).

V. SOLITON STABILITY

The value of S^z is positive and, in some sense, it can be considered as a measure of the power of the soliton; a larger soliton amplitude and characteristic size corresponds to a larger value of S^z. In particular, the vanishing of S^z corresponds to the disappearance of the soliton which is obviously the case in the absence of antidamping effects caused by spin current. The stationary points found in the previous section correspond to the mutual compensation of damping and antidamping effects for some concrete values of soliton parameters. The stability of the soliton is determined by anal-

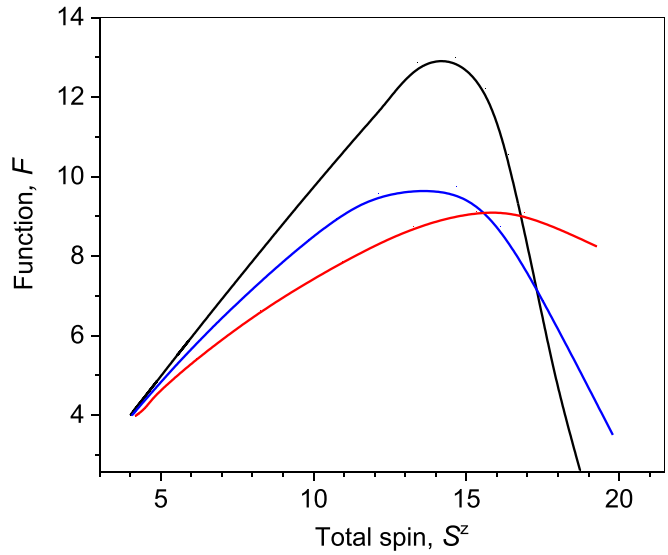

FIG. 6. The integral, F versus S^z: $\bar{\nu} = 1$ (black), $\bar{\nu} = 0.5$ (blue), and $\bar{\nu} = 0.1$ (red).

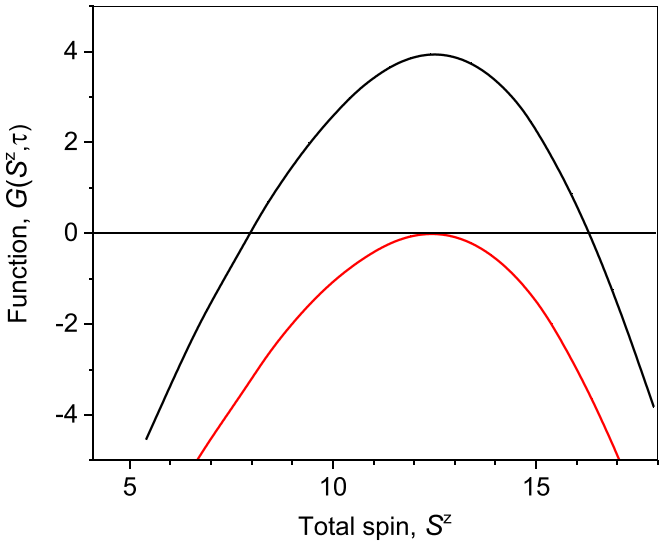

FIG. 7. The function $G(S^z, 4)$ for $\bar{\nu} = 0.5$ in the region of the critical points (upper black curve), and $G(S^z, 3.476)$ at the minimum sustaining torque, $\tau_{s,\min}$ (lower red curve).

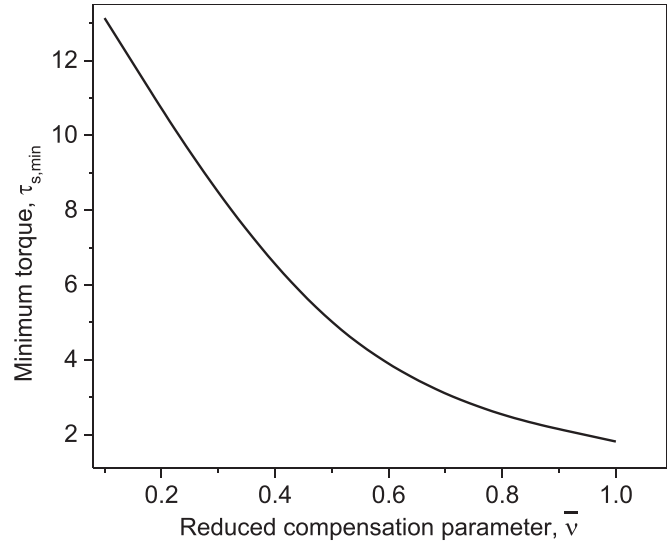

FIG. 8. $\tau_{s,\min}$ versus $\bar{\nu}$ over the range $0.1 \leqslant \bar{\nu} \leqslant 1$.

ysis of the critical points of Eq. (10) where the right-hand side is now expressed as a function of the independent variable S^z calculated from Eq. (10). It is convenient to define the right-hand side of Eq. (10) as the function

$$G(S^z, \tau) = -\alpha\bar{\omega}\sqrt{\omega_{\rm ex}\omega_K}J + \tau p_3 F, \tag{13}$$

where the units are GHz. The integral J is expressed as a function of S^z through multiplication of Eq. (6) by $\rho\theta_\rho$ and integration over the free-layer area to obtain the relation

$$S^z = 2J\bar{\omega}/(1+\bar{\omega}^2). \tag{14}$$

Since $\bar{\omega}$ can be expressed as a function of S^z, Eq. (14) is used to obtain the integral $J(S^z)$ to be used in Eq. (13).

Stability can be determined by time integration of Eq. (10) at the stationary point $G(S^z, \tau) = 0$ indicating that the soliton is stable if $dG/dS^z < 0$ and unstable if $dG/dS^z > 0$. The particular value of τ at this point is referred to as the sustaining torque. As an example, consider a sustaining torque of $\tau = 4$ GHz for $\bar{\nu} = 0.5$ with the function $G(S^z, 4)$ plotted in Fig. 7. It is also noted that as τ is decreased the stable point moves to a larger S^z and the maximum of $G(S^z, \tau)$ decreases to a point where the maximum is tangent to the S^z axis defining the minimum sustaining torque, $\tau_{s,\min}$.

The shape of the curves in Fig. 7 is understood by referring to the forms of the function defining $G(S^z, \tau)$ in Eq. (13). From numerical calculations it is noted that the product $\bar{\omega}(S^z)J(S^Z)$ is a monotonically increasing function for larger values of S^Z. However, $F(S^z, \tau)$ has a maximum depending on $\bar{\nu}$ as in Fig. 6, implying that the maximum as well as both critical points are the result of the limiting values for $\theta(0)$. It is also noted that the stable critical point will be stable for any large enough value of τ. In Fig. 7 notice that there are two critical points at $S^z = 7.962$ and $S^z = 16.343$ with the second point being stable. The stable critical point corresponds to $\bar{\omega} = 0.354$ and $\Omega = 0.202$ with a corresponding $\theta(0) = 0.983\pi$. By finding the tangent point on the S^z axis as in Fig. 7, the minimum sustaining torque is obtained for any reduced compensation parameter as noted in Fig. 8. In general, it is seen that as $\bar{\nu}$ increases, $\tau_{s,\min}$ decreases.

Using this method, the reduced frequency can be obtained for a sustaining torque for various values of the reduced compensation parameter. Next consider the dependence of the reduced frequency on the sustaining spin torque. These results are seen in Fig. 9 for three values of the reduced compensation parameter.

It is noted that each curve starts at the minimum sustaining torque for each value of $\bar{\nu}$ and ends at the minimum value of S^z calculated from Eq. (10), which is determined by the minimum $\theta(0) = 0.4\pi$ selected for calculation of these data. For the ferromagnetic case, early indirect experimental detection [19] of magnon drop solitons indicated a very weak increase of the frequency with an increase in the nanocontact current. On the other hand, simulations [8] including effects of the Oersted field showed a small frequency decrease as

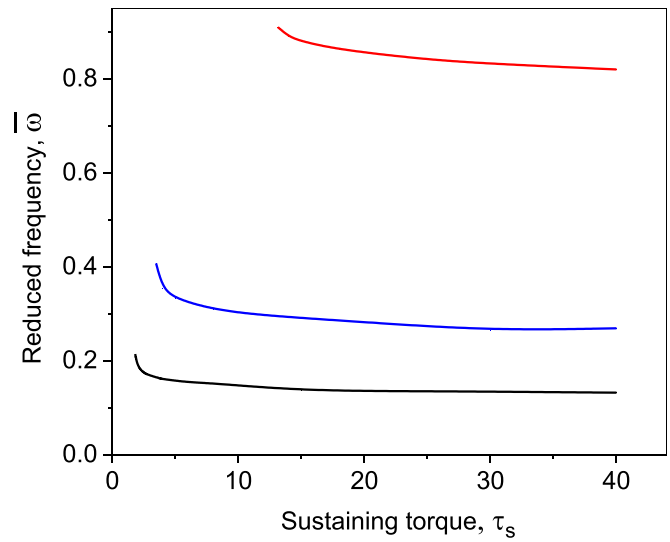

FIG. 9. Reduced frequency versus sustaining torque, τ_s : $\bar{\nu} = 1$ (black), $\bar{\nu} = 0.5$ (blue), and $\bar{\nu} = 0.1$ (red).

the nanocontact current is increased. Here a sharp frequency decrease is noticed as the torque is increased from $\tau_{s,\min}$, a gradual decrease as the torque is decreased further for all values of the compensation parameter, and the frequency approaches a constant value at high τ. The general tendency is the smaller the value of $\bar{\nu}$, the larger the reduced frequency. Thus, the small values of decompensation parameter $\bar{\nu} < 0.1$ are very attractive for the obtaining of higher frequencies, but the minimal sustaining torque also increases for smaller $\bar{\nu}$, so it is necessary to estimate values of τ corresponding to typical nanocontact current densities. First let us discuss the relation between the sustaining torque and frequency at the $\bar{\nu} \to 0$ limit where the scale parameter a is undefined, but $\bar{\omega} \to 1$ and Fig. 8 implies that the minimum sustaining torque becomes very large. To determine if these torques correspond to typical current densities in nanocontacts, current densities are estimated using $\tau = \sigma j$ from Sec. II. In the determination of σ the saturation magnetization is determined from the anisotropy frequency to be $M_s = 0.66 \times 10^5$ A/m, $g = 2.2$, $\epsilon = 0.2$, and $L = 5$ nm. The numerical value for the coefficient is $\sigma = 0.0386\ \mathrm{m}^2/\mathrm{C}$. Then for the 50 nm radius nanocontact and $\tau = 40$ GHz the current density is $j = 6.5 \times 10^{12} \mathrm{A/m}^2$, which is a large current density for a typical nanocontact. Both Figs. 8 and 9 show that as $\bar{\nu} \to 0$ the value of $\tau_{s,\min}$ becomes very large, implying that current density will become too large. Therefore, this limit is not attainable in typical applications. In fact, for the parameters used here only values of $\tau < (10-15)$ GHz are acceptable that go with the values of $\bar{\nu} > (0.1-0.2)$ considered here with a corresponding reduced frequency $\bar{\omega}$ of about 0.5. It is further noted that the values $\bar{\nu} \sim 1$ already correspond to a high level of compensation, $(s_1 - s_2)/(s_1 + s_2)\tilde{}\sqrt{\omega_{\mathrm{ex}}/\omega_K} = 0.024$, with full manifestation of noncompensated ferrimagneticlike dynamics and high frequencies of the order of the exchange-enhancement "antiferromagnetic" limit value $\sqrt{\omega_{\mathrm{ex}}/\omega_K}$.

VI. CONCLUSION

In this article conservative and dissipative magnon drop solitons are investigated in the two-sublattice ferrimagnet near the angular compensation point. For the case of the conservative soliton, rescaling of parameters leads to the same equation to be solved for the conservative soliton in the ferromagnet with a dimensionless-frequency-like parameter Ω. Close to the compensation point, i.e., at $\bar{\nu} < 0.2$, the precession frequency in the soliton is comparable to the antiferromagnetic resonance frequency, which is in the subterahertz region [18], whereas at $\bar{\nu} \gg 1$, the frequency decreases to the range of dozens of GHz as the lower mode of magnetic resonance for ferrimagnets far from the compensation. Analytical expression for the frequency is obtained as a function of the compensation parameter, ν and Ω.

The dissipative soliton includes Gilbert damping, which is countered by spin-torque antidamping resulting in stable soliton structures. For this case it is necessary to determine the stability of the soliton defined as the point in parameter space where the total z component of the magnetization remains constant. The stability analysis leads to a determination of the sustaining value of the spin torque as well as the minimum sustaining spin torque above which stable solitons can form. Finally, estimates of the sustaining current density are calculated for typical ferromagnetic TM-RE alloys.

ACKNOWLEDGMENT

This work is partly supported by the National Research Fund of Ukraine within Project No. 2020.02/026.

[1] A. A. Belavin and A. M. Polyakov, Metastable states of two-dimensional isotropic ferromagnets, JETP Lett. **22**, 245 (1975).
[2] B. A. Ivanov and A. M. Kosevich, Bound states of a large number of magnons in a three-dimensional ferromagnet (magnon drops), JETP Lett. **24**, 454 (1976).
[3] A. M. Kosevich, B. A. Ivanov, and A. S. Kovalev, Nonlinear localized magnetization wave of a ferromagnet as a bound state of a large number of magnons, JETP Lett. **25**, 486 (1977).
[4] A. S. Kovalev, A. M. Kosevich, and K. V. Maslov, Magnetic vortex-topological soliton in a ferromagnet with an easy-axis anisotropy, JETP Lett. **30**, 321 (1979).
[5] A. M. Kosevich, B. A. Ivanov, and A. S. Kovalev, Magnetic solitons, Phys. Rep. **194**, 117 (1990).
[6] V. P. Voronov, B. A. Ivanov, and A. M. Kosevich, Two-dimensional topological solitons in ferromagnets, Zh. Eksp. Teor. Fiz. **84**, 2235 (1983).
[7] K. L. Metlov, Magnetization Patterns in Ferromagnetic Nanoelements as Functions of Complex Variable, Phys. Rev. Lett. **105**, 107201 (2010).
[8] M. A. Hoefer, T. J. Silva, and M. W. Keller, Theory for a dissipative droplet soliton excited by a spin torque nanocontact, Phys. Rev. B **82**, 054432 (2010).
[9] L. D. Bookman and M. A. Hoefer, Analytical theory of modulated magnetic solitons, Phys. Rev. B **88**, 184401 (2013).
[10] S.-B. Choe, Y. Acremann, A. Scholl, A. Bauer, A. Doran, J. Stöhr, and D. C. Padmore, Vortex core-driven magnetization dynamics, Science **304**, 420 (2004).
[11] V. S. Pribiag, I. N. Krivorotov, G. D. Fuchs, P. M. Braganca, O. Ozatay, J. C. Sankey, D. C. Ralph, and R. A. Buhrman, Magnetic vortex oscillator driven by d.c. spin-polarized current, Nat. Phys. **3**, 498 (2007).
[12] M. R. Pufall, W. H. Rippard, M. L. Schneider, and S. E. Russek, Low-field current-hysteretic oscillations in spin-transfer nanocontacts, Phys. Rev. B **75**, 140404(R) (2007).
[13] Q. Mistral, M. van Kampen, H. Hrkac, J.-V. Kim, T. Devolder, P. Crozat, C. Chappert, L. Lagae, and T. Schrefl, Current-Driven Vortex Oscillations in Metallic Nanocontacts, Phys. Rev. Lett. **100**, 257201 (2008).
[14] R. Lehndorff, D. E. Bürgler, S. Gliga, R. Hertel, P. Grünberg, C. M. Schneider, and Z. Celinski, Magnetization dynamics in spin-torque nano-oscillators: Vortex state versus uniform state, Phys. Rev. B **80**, 054412 (2009).
[15] S. Petit-Watelot, J.-V. Kim, A. Ruotolo, R. M. Otxoa, K. Bouzehouane, J. Grollier, A. Vansteenkiste, B. Van de Wiele,

V. Cros, and T. Devolder, Commensurability and chaos in magnetic vortex oscillations, Nat. Phys. **8**, 682 (2012).

[16] C. D. Stanciu, A. V. Kimel, F. Hansteen, A. Tsukamoto, A. Itoh, A. Kiriliyuk, and Th. Rasing, Ultrafast spin dynamics across compensation points in ferrimagneticGdFeCo: The role of angular momentum compensation, Phys. Rev. B **73**, 220402(R) (2006).

[17] K.-J. Kim, S. K. Kim, Y. Hirata, S.-H. Oh, T. Tono, D.-H. Kim, T. Okuno, W. S. Ham, S. Kim, G. Go, Y. Tserkovnyak, A. Tsukamoto, T. Moriyama, K.-J. Lee, and T. Ono, Fast domain wall motion in the vicinity of the angular momentum compensation temperature offerrimagnets, Nat. Mater. **16**, 1187 (2017).

[18] I. Lisenkov, R. Khymyn, J. Åkerman, N. X. Sun, and B. A. Ivanov, Sub terahertz ferromagnetic spin-torque oscillator, Phys. Rev. B **100**, 100409(R) (2019).

[19] R. Mishra, J. Yu, X. Qiu, M. Motapothula, T. Venkatesan, and H. Yang, Anomalous Current-Induced Spin Torques in Ferrimagnets near Compensation, Phys. Rev. Lett. **118**, 167201 (2017).

[20] S. K. Kim and Y. Tserkovnyak, Fast vortex oscillations in a ferromagnetic disk near the angular momentum compensation point, Appl. Phys. Lett. **111**, 032401 (2017).

[21] C. E. Zaspel, E. G. Galkina, and B. A. Ivanov, High-Frequency Current-Controlled Vortex Oscillations in Ferrimagnetic Disks, Phys. Rev. Appl. **12**, 044019 (2019).

[22] S. M. Mohseni, S. R. Sani, J. Persson, T. M. A. Nguyen, S. Chung, Y. Pogoryelov, P. K. Muduli, E. Iacocca, A. Eklund, R. K. Dumas, S. Bonetti, A. Deac, M. A. Hoefer, and J. Åkerman, Spin torque—generated magnetic droplet solitons, Science **339**, 1295 (2013).

[23] D. Backes, F. Macià, S. Bonetti, R. Kukreja, H. Ohldag, and A. D. Kent, Direct Observation of a Localized Magnetic Soliton in a Spin-Transfer Nanocontact, Phys. Rev. Lett. **115**, 127205 (2015).

[24] S. Chung, A. Eklund, E. Iacocca, S. M. Mohseni, S. R. Sani, L. Bookman, H. A. Hoefer, R. K. Dumas, and J. Åkerman, Magnetic droplet nucleation boundary in orthogonal spin-torque nano-oscillators, Nat. Commun. **7**, 11209 (2016).

[25] B. A. Ivanov, Ultrafast spin dynamics and spintronics for ferrimagnets close to the spin compensation point (Review), Low Temp. Phys. **45**, 935 (2019).

[26] E. A. Turov, A. V. Kolchanov, M. I. Kurkin, I. F. Mirsaev, and V. V. Nikolaev, *Symmetry and Physical Properties of Antiferromagnets* (Cambridge International Science Publishing Ltd., Cambridge, 2010), p. 570.

[27] D. Raasch, J. Reck, C. Mathieu, and B. Hillebrands, Exchange stiffness constant and wall energy density of amorphous GdTbFeCo thin films, J. Appl. Phys. **76**, 1145 (1994).

[28] E. G. Galkina, C. E. Zaspel, B. A. Ivanov, N. E. Kulagin, and L. M. Lerman, Limit velocity and dispersion law for domain walls in ferrimagnets in the vicinity of the spin compensation point, JETP Lett. **110**, 481 (2019).

[29] I. V. Bar'yakhtar and B. A. Ivanov, Dynamic solitons in a uniaxial antiferromagnet, Zh. Eksp. Teor. Fiz. **85**, 328 (1983).

[30] E. G. Galkina and B. A. Ivanov, Dynamical solitons in antiferromagnets (Review article), Low Temp. Phys. **44**, 618 (2018).